J Mater Sci (2011) 46:7511–7516
DOI 10.1007/s10853-011-5722-2

Encapsulation of α-cyano-4-hydroxycinnamic acid into a NaY zeolite

Natália Vilaça · Ricardo Amorim · Olga Martinho · Rui M. Reis · Fátima Baltazar · António M. Fonseca · Isabel C. Neves

Received: 6 May 2011 / Accepted: 14 June 2011 / Published online: 29 June 2011

Abstract The faujasite zeolite structure was studied to investigate its suitability for development of new drug delivery systems (DDS). The sodium form (NaY) of the zeolite was used for encapsulation of α-cyano-4-hydroxycinnamic acid (CHC), an experimental anticancer drug used in colorectal cancer therapy. The DDS was prepared by diffusion in liquid phase of CHC as a guest in the void space of the host zeolite structure at pH 7.0. The molecular integrity of CHC in the encapsulation process was evaluated by proton nuclear magnetic resonance spectroscopy (^{1}H NMR) and Ultraviolet–Visible spectroscopy (UV–Vis). The new drug delivery system, CHC@NaY, was characterized by Fourier transform infrared spectroscopy and UV–Vis, chemical analysis, powder X-ray diffraction, and Scanning electron microscopy. Analysis of the data of the drug alone and encapsulated in NaY show that CHC and the zeolite framework preserved their original structure. The effect of the zeolite and DDS on HCT-15 human colon carcinoma cell line viability was evaluated. The encapsulation of CHC significantly increased its potency.

N. Vilaça · A. M. Fonseca · I. C. Neves (✉)
Centre of Chemistry, Chemistry Department, University of Minho, Campus de Gualtar, 4710-057 Braga, Portugal
e-mail: ineves@quimica.uminho.pt

R. Amorim · O. Martinho · R. M. Reis · F. Baltazar
Life and Health Sciences Research Institute (ICVS), School of Health Sciences, University of Minho, Braga, Portugal

R. Amorim · O. Martinho · R. M. Reis · F. Baltazar (✉)
ICVS/3B's-PT Government Associate Laboratory, Braga/Guimarães, Portugal
e-mail: fbaltazar@ecsaude.uminho.pt

R. M. Reis
Molecular Oncology Research Center, Barretos Cancer Hospital, Barretos, SP, Brazil

Introduction

Due to biological properties and stability in biological environments, zeolite structures have a great potential for medical use. Zeolites have been examined as carriers for slow or delayed release of anthelmintic and antitumoral drugs. The latest experimental studies, based on the results obtained in various tumor cells and in tumor bearing animals, have shown that zeolites can be successfully used as adjuvants in anticancer therapy. Zeolite nanocrystals have been used in the enrichment of low abundance peptides/proteins as well as in the immobilization of enzymes for biosensing and for processes by magnetic resonance imaging [1]. Zeolites are crystalline solids with very regular microporous structures in which active chemical interesting compounds can be included. Zeolites have broad applications in heterogeneous catalysis, textile manufacturing, polymer catalytic degradation, electrochemical properties, and have also attracted interest in material sciences for the development of functional materials and in nanotechnology [2–15].

In this study, we report the use of the zeolite structure for drug delivery systems (DDS). The host zeolite has a faujasite (FAU) framework based on sodalite cages that are joined by oxygen bridges between the hexagonal faces. Eight sodalite cages are linked together, forming a large central cavity or supercage with a diameter of 1.18 nm. The supercages share a 12-membered ring with an open diameter of 0.74 nm [16–18] (Fig. 1).

Encapsulation of α-cyano-4-hydroxycinnamic acid (CHC) was prepared by diffusion in liquid phase in the

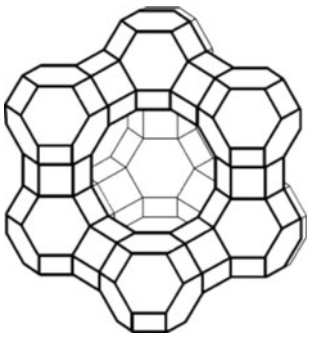

Fig. 1 Faujasite structure of NaY zeolite [16]

void space of the host zeolite NaY. The new drug delivery system, CHC@NaY, was characterized by spectroscopic techniques (Fourier transform infrared (FTIR), proton nuclear magnetic resonance spectroscopy (^{1}H NMR), and Ultraviolet–Visible spectroscopy (UV–Vis)), chemical analysis, powder X-ray diffraction (XRD), and scanning electron microscopy (SEM). The experimental anticancer drug α-cyano-4-hydroxycinnamic acid (CHC), here used as a model for colon carcinoma treatment [19–22], was chosen as the guest compound in the zeolite for drug delivery systems. To the best of our knowledge, there are no studies using zeolites as DDS for anticancer drugs [1, 23]. The new DDS was evaluated on HCT-15 human colon carcinoma cell viability. This study is a contribution for the development of a new DDS based in zeolites in the cancer context.

Experimental

Materials and reagents

The zeolitic structure is commercially available; FAU zeolite in powder form (CBV100) was obtained from Zeolyst International. The zeolite in sodium form was previously dehydrated at 120 °C overnight in an oven. CHC was purchased from Sigma-Aldrich and used as received. Acetone, the solvent used for encapsulation in this study, was purchased from Merck (analytical grade). Human colon carcinoma-derived cell line HCT-15 was kindly provided by Dr. Raquel Seruca (IPATIMUP, Porto, Portugal).

Encapsulation of CHC in NaY

The encapsulation of CHC in NaY has been described elsewhere [23]: 500 mg of NaY was reacted with a solution of 49.20 mg CHC in acetone (15 mL), as a solvent. This mixture was carried out by stirring at room temperature for 48 h. During this time, the original white color of NaY changed to the characteristic color of the CHC, yellow, indicating that the drug species was effectively entrapped inside the host. This finding was also confirmed by the disappearance of the yellow color of the starting CHC solution after 3 h in contact with the zeolite and the efficiency of the encapsulation was screened by HPLC. The load of drug within the zeolite and on the surface was determined by gravimetric analysis.

Characterization

Room temperature FTIR spectra of the samples in KBr pellets were measured using a Bomem MB104 spectrometer in the range 4000–500 cm^{-1} by averaging 20 scans at a maximum resolution of 4 cm^{-1}. Chemical analysis of C, H, and N was carried out on a Leco CHNS-932 analyzer. ^{1}H NMR spectra were obtained on a Varian Unity Plus Spectrometer at an operating frequency of 300 MHz using the solvent peak as internal reference at 25 °C, chemical shifts of protons being given in ppm using δ_H $Me_4Si = 0$ ppm as reference. The electronic UV–Vis absorption spectrum of the residual solutions was obtained in acetone. UV–Vis spectra of the drug molecule and the suspension of NaY and CHC@NaY in Nujol were collected in a Shimadzu UV/2501PC spectrophotometer using quartz cells at room temperature. Phase analysis was performed by XRD using a Philips PW1710 diffractometer. Scans were taken at room temperature in a 2θ range between 5° and 60°, using Cu-Kα radiation. SEM was collected on a LEICA Cambridge S360 Scanning Microscope equipped with an EDX system (semi-quantitative analysis with detection limits of ~1.0 weight % for most elements). In order to avoid surface charging, samples were coated with gold in vacuum prior to analysis, by using a Fisons Instruments SC502 sputter coater. Images of the cells and the DDS during the drug bioactivity studies were obtained in an optical inverted microscope (Olympus IX51). The analysis was carried out by high performance liquid chromatography (HPLC–JASCO 980-PU) using an isocratic pump and a double on line detection including an UV–Vis detector and refractometer.

Drug release studies

HCT-15 colon carcinoma cells were maintained in RPMI 1640 medium (Gibco), supplemented with 10% (v/v) fetal bovine serum (FBS) (Gibco, Invitrogen, USA), and 1% (v/v) penicillin–streptomycin solution (P/S) (Invitrogen, USA) and incubated at 37 °C in a 5% CO_2 humidified atmosphere. Cells were subcultured approximately every 3 days and maintained in a log-phase growth. Cell viability was assessed using the In Vitro Toxicology Assay Kit, Sulforhodamine B based (Sigma-Aldrich). HCT-15 cells were seeded in 96-well plates (5000 cells/100 μL/well) and incubated at 37 °C in a 5% CO_2 humidified atmosphere for 24 h. In order

to assess the effects of NaY and CHC@NaY, the spent media were discarded and cells were incubated with increasing concentrations of the systems in new culture medium. Controls were performed with culture medium alone. After an incubation period of 24 h, the spent media were removed and the plate wells were washed with 1× phosphate buffered saline, pH 7.4. After a fixation step with cold 10% Trichloroacetic acid, cells were stained with 0.4% Sulforhodamine B and the incorporated dye were solubilized with Sulforhodamine B assay solubilization solution (10 mM Tris). Absorbance was monitored with a microplate reader at 570 nm with a background absorbance of 655 nm. Cell viability was determined as percent viability: (OD experiment/OD control) × 100 (%).

Results and discussion

An experimental anticancer drug (CHC) was used for preparation of a new DDS based on a NaY zeolite which was modified by trapping the drug molecule into its framework in liquid phase at pH 7.

The length between the OH group from the aryl ring and COOH is approximately 10.6 Å in the planar and linear CHC molecule. However, the aryl ring is 5.9 Å, suggesting that this drug can easily diffuse into the structure of the NaY zeolite.

Loading of the CHC molecule into zeolite NaY was determined by gravimetric analysis. The initial amount of CHC used for encapsulation was 25.9×10^{-2} mmol. After preparation of DDS, CHC loading in NaY was 22.6×10^{-2} mmol, indicating that 87.3% of the CHC initially present has been retained inside the zeolite.

The yield of the CHC encapsulation was confirmed by the analytical data of carbon and nitrogen content obtained by elemental analysis (Table 1).

The C/N ratio of the encapsulated CHC, obtained by chemical analysis, was similar to the theoretically expected C/N ratio of CHC, indicating the presence of the molecular drug structure inside the zeolite. The UV/Vis absorption spectra of NaY zeolite and the DDS was used as a tool to study the encapsulation of the drug molecule in the host zeolite (Fig. 2).

The UV/Vis absorption spectrum of CHC@NaY display bands which are not shown in the spectrum of the zeolite host (Fig. 2a, c). The spectrum of CHC (Fig. 2b) measured

Table 1 Elemental composition of CHC and DDS

Samples	C (%)	N (%)	C/N
CHC	63.49	7.40	8.6
CHC@NaY	11.45	1.31	8.7

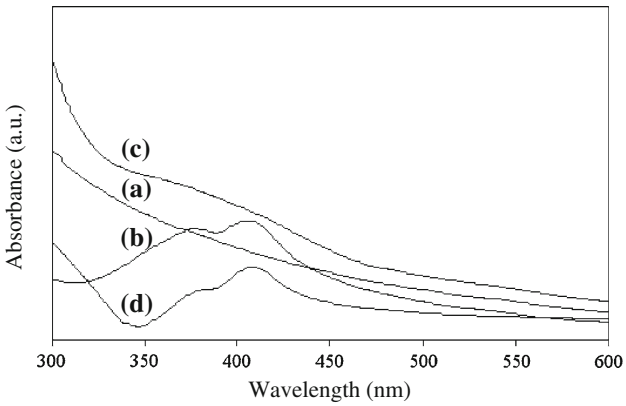

Fig. 2 UV/vis spectra of the samples: (*a*) NaY, (*b*) CHC, (*c*) CHC@NaY and (*d*) CHC@NaY without the matrix obtained in Nujol suspensions

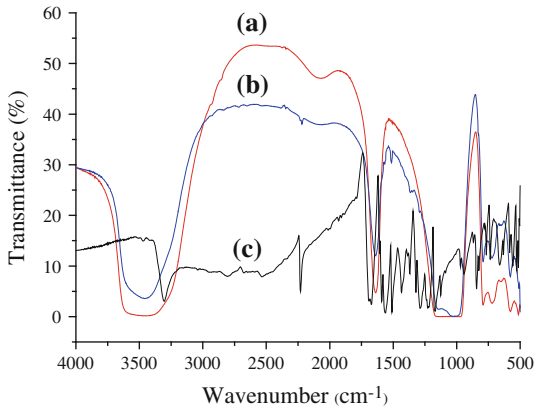

Fig. 3 FTIR spectra of the samples: (*a*) NaY, (*b*) CHC and (*c*) CHC@NaY

in Nujol at room temperature, exhibited two bands at 370 and 415 nm. The spectra of CHC@NaY exhibited similar bands to CHC (Fig. 2b, d). However, the control in residual solutions during the preparation, by ^{1}H NMR and UV–Vis spectroscopy, confirms that CHC after encapsulation in NaY is in its neutral form.

The data obtained by vibrational spectroscopy can provide structural information of the host framework and the encapsulated drug molecule. Figure 3 shows the infrared spectra in the range 4000–600 cm^{-1} of NaY (a), CHC (b), and CHC@NaY (c).

The FTIR spectra of the guest compound and the host presented in Fig. 3 are dominated by the strong bands assigned to the vibration of zeolite structure. The presence of physisorbed water is detected by the ν(O–H) stretching vibration at 3450 cm^{-1} and the ν(O–H) deformation band at 1640 cm^{-1}. The bands corresponding to the lattice vibrations are observed in the spectral region between 1300 and 450 cm^{-1} [7, 8]. No shift or broadening of the zeolite vibrations bands are observed upon inclusion of the CHC,

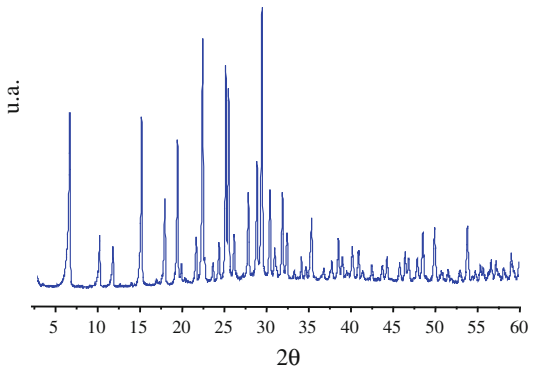

Fig. 4 XRD pattern of CHC@NaY

which provides further evidence that the zeolite structure remains unchanged after encapsulation.

In addition to these strong bands caused by the host matrix, the FTIR spectrum of CHC@NaY show bands in the 2300–2000 and 1600–1200 cm^{-1} regions where NaY does not absorb and they are attributed to the presence of the encapsulated drug. This means that the zeolite framework does not interfere with the IR absorption of the incorporated guest. Comparison of the spectra of the encapsulated CHC with the parent drug molecule provides evidence for the entrapping of CHC in NaY.

The spectrum of CHC shows the characteristic bands of the drug: 3308 (νOH), 2224 (νCN), 1669 (νC=O), and 1567–1295 cm^{-1} attributed to C–C and C–H bands. The spectra of the encapsulated drug as well as CHC alone showed similar bands. The spectrum of CHC@NaY shows bands due to the drug molecule at 2225, 1560, 1502, 1362, and 1291 cm^{-1} indicating no host–guest interactions. Furthermore, from elemental analysis, UV–Vis, and FTIR data, we observed that the zeolitic environment preserves the molecular structure of the drug.

FTIR analysis was an important tool also for obtaining the framework Si/Al ratio of the FAU zeolite [24, 25]. The most sensitive band in the zeolite Y structure can be observed at 570 and 600 cm^{-1} and was used to calculate the framework Si/Al ratio (Eq. 1):

$$x = 3.857 - 0.00621 w_{DR}(cm^{-1}), \quad (1)$$

where $x = [1 + (Si/Al)]^{-1}$, with $0.1 < x < 0.3$, and w_{DR} is the zeolite specific double ring vibration mode in the range 570–600 cm^{-1}. The obtained framework Si/Al ratio was 2.83 and 2.80 for NaY and DDS, respectively.

Structural characterization of NaY and CHC@NaY was obtained by XRD. The position and intensity of the observed XRD patterns of the samples remained unchanged after CHC encapsulation. Figure 4 shows the CHC@NaY XRD pattern.

The relative crystallinity was estimated by comparing the intensities of CHC@NaY with those of starting NaY as a standard sample (100% crystalline). The total intensities of the six peaks assigned to [331], [511], [440], [533], [642], and [555] reflections were used for the comparison, according to ASTM D 3906-80 method. After encapsulation of CHC, CHC@NaY maintained over 90% of crystallinity when compared to the respective standard NaY zeolite. XRD data can be used to estimate particle size by using the Debye–Scherrer equation [8]. The average particle size of the zeolite was estimated from the characteristic reflection peak [26]. The prepared DDS shows the same order of magnitude particle size, which gives an evidence for the preservation of the zeolite structure (50.0 nm for NaY and 57.8 nm for CHC@NaY).

Likewise, XRD analysis allows the determination of the framework's Si/Al ratio. The ratio was obtained by the calculated unit cell parameters using the Breck and Flanigen equation (Eq. 2) [27]:

$$N_{Al} = 115.2\ (a_0 - 24.191), \quad (2)$$

where N_{Al} is the framework's aluminum number and a_0 is the cell parameter. The unit cell parameters were calculated from the values of [533], [642], and [555] reflection peaks according to the ASTM D 3942-80 method. The calculated framework Si/Al ratios were 2.80 for NaY and 2.78 for DDS.

The total Si/Al ratio of the starting zeolite and DDS was determined by chemical analysis (ICP-AES): 2.83 for NaY and 2.84 for DDS. The values of the Si/Al ratios obtained by ICP-AES and the framework Si/Al ratios calculated by XRD and FTIR show that encapsulation of the drug does not affect the zeolite structure and has a regular distribution of silicon and aluminum throughout the zeolite structure.

In order to evaluate the morphology of the zeolite after encapsulation of CHC, SEM micrographs were obtained (Fig. 5).

The resulting SEM micrographs show that NaY and DDS have similar morphology, typical of the FAU structure, with regular small particles. However, in DDS, the energy-dispersive X-ray analysis plots detected the presence of nitrogen from the CHC molecule on the spotted surface.

HCT-15 human colon carcinoma cell viability was evaluated using the new DDS. The results show that CHC@zeolite has a significantly higher inhibitory effect on HCT-15 cell viability when compared to CHC alone. Drug bioactivity studies with NaY and CHC@NaY were performed with 0.05 mg/mL of DDS by diluting the DDS stock suspension (0.50 mg/mL) in culture medium (RPMI 460). For higher CHC@zeolite concentrations, the amount of DDS compromised the access of medium components by the cells (Fig. 6).

Our results show that zeolite NaY is not toxic to the cells for the selected period of incubation and

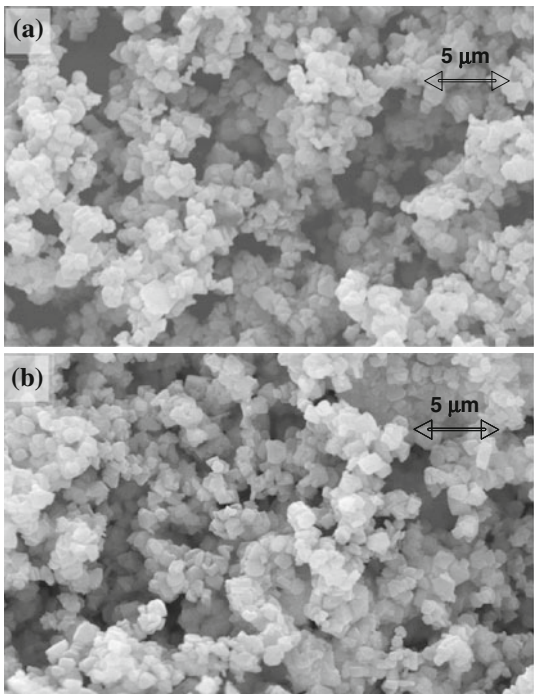

Fig. 5 Scanning electron microscopy (SEM) images of NaY (**a**) and CHC@NaY with same resolution (×5000)

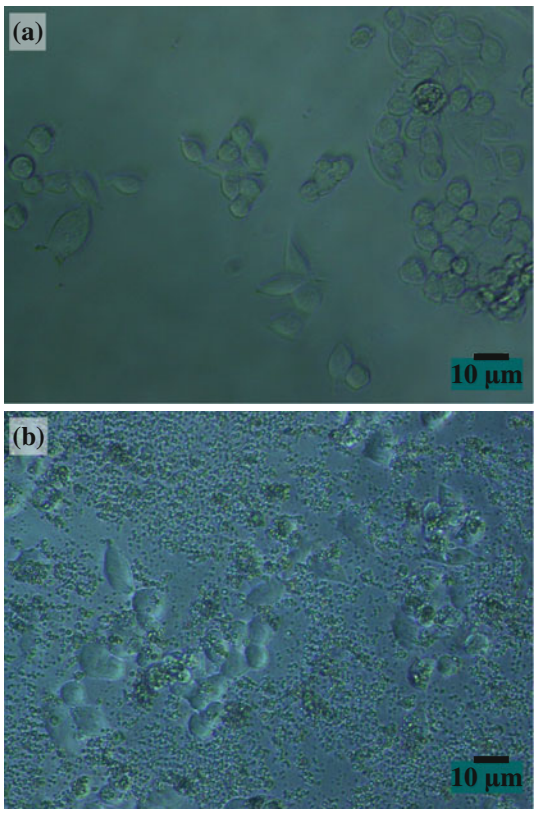

Fig. 6 Optical microscopy images taken in an inverted optical microscope of (**a**) HCT-15 cells and 0.50 mg/mL of (**b**) DDS

concentrations. By comparing the results obtained when treating HCT-15 cells with the non-encapsulated CHC with the results obtained for CHC@NaY, there is an obvious potentiation of the effect of the drug. About 6 mM of the non-encapsulated drug are necessary for a 30% of inhibition (IC30) in cell viability. In contrast, only 0.054 mM of the encapsulated drug produces the same magnitude of inhibition, corresponding to a potentiation of the drug effect of about 110-fold.

Conclusions

Combining spectroscopic techniques and chemical analysis provides a powerful tool to reveal the unequivocal evidence for the encapsulation of CHC in the framework structure of zeolite NaY.

In the light of the obtained results, it can be concluded that CHC molecule can be encapsulated in NaY zeolite supercages, without structural modification or loss of crystallinity of the zeolite framework, while the drug molecule retains its molecular integrity.

Importantly, CHC@NaY led to an inhibition of cell viability up to 110-fold when compared to the non-encapsulated drug. These results indicate the potential of the zeolites for drug loading and delivery to cancer cells. It would be important in the near future to test other CHC/zeolite ratios and also the encapsulation of CHC in different zeolite structures.

Acknowledgements The authors are thankful to Dr. K. Biernacki for DFT calculations and Dr. A.S. Azevedo for collecting the powder diffraction data. OM and RA are recipients of fellowships (SFRH/BD/36463/2007, SFRH/BI/51118/2010) from Fundação para a Ciência e a Tecnologia (FCT, Portugal).This study was supported by the Centre of Chemistry and Life and Health Sciences Research Institute (ICVS), University of Minho, Portugal, FCT (Portugal) through POCTI and FEDER projects (ref. POCTI-SFA-3-686) and by the FCT grant ref. PTDC/SAU-FCF/104347/2008, under the scope of "Programa Operacional Temático Factores de Competitividade" (COMPETE) of "Quadro Comunitário de Apoio III" and co-financed by Fundo Comunitário Europeu FEDER.

References

1. Danilczuk PM, Dugopolska K, Ruman T, Pogocki D (2008) Mini Rev Med Chem 8:1407
2. Corma A, Garcia H (2004) Eur J Inorg Chem 6:1143
3. Kuzniarska-Biernacka I, Biernacki K, Magalhães AL, Fonseca AM, Neves IC (2011) J Catal 278:102
4. Parpot P, Teixeira C, Almeida AM, Ribeiro C, Neves IC, Fonseca AM (2009) Microporous Mesoporous Mater 117:297
5. Neves IC, Botelho G, Machado AV, Rebelo P, Ramôa S, Pereira MFR, Ramanathan A, Pescarmona P (2007) Polym Degrad Stab 92:1513
6. Van Santen RA, Kramer GJ (1995) Chem Rev 95:637

7. Neves IC, Cunha C, Pereira MR, Pereira MFR, Fonseca AM (2010) J Phys Chem C 114:10719
8. Lopes AC, Silva MP, Gonçalves R, Pereira MFR, Botelho G, Fonseca AM, Lanceros-Mendez S, Neves IC (2010) J Phys Chem C 114:14446
9. Abbo HS, Titinchi SJJ (2010) Top Catal 53:1401
10. Yang Y, Ding H, Hao S, Zhang Y, Kan Q (2011) Appl Organometal Chem 25:262
11. Perez E, Martin L, Rubio C, Urieta JS, Piera E, Caballero MA, Tellez C, Coronas J (2010) Ind Eng Chem Res 49:8495
12. Talebi J, Halladj R, Askari S (2010) J Mater Sci 45:3318. doi: 10.1007/s10853-010-4349-z
13. Gomes R, Albuquerque RQ, Pina F, Parola J, De Cola L (2010) Photochem Photobiol Sci 9:991
14. Lang JW, Kong LB, Wu WJ, Luo YC, Kang L (2009) J Mater Sci 44:4466. doi:10.1007/s10853-009-3677-3
15. Nethravathi BP, Mahendra KN, Reddy KRK (2011) J Porous Mater 18:389
16. Database of zeolite structures from the International Zeolite Association (IZA-SC). www.iza-structure.org/databases/. Accessed 03 Apr 2011
17. Baerlocher Ch, McCusker LB, Olson DH (2007) Atlas of zeolite framework types, sixth revised edition. Elsevier, Amsterdam
18. Subhash B (1990) Zeolite catalysis: principles, applications. CRC Press, Inc., Boca Raton
19. Halestrap AP, Meredith D (2004) Eur J Physiol 447:619
20. Pinheiro C, Longatto-Filho A, Scapulatempo C, Ferreira L, Martins S, Pellerin L, Rodrigues M, Alves VAF, Schmitt F, Baltazar F (2008) Virchows Arch 452:139
21. Pinheiro C, Longatto-Filho A, Pereira SMM, Etlinger D, Moreira MAR, Jubé LF, Queiroz GS, Schmitt F, Baltazar F (2009) Dis Marker 26:97
22. Pinheiro C, Albergaria A, Paredes J, Sousa B, Dufloth R, Vieira D, Schmitt F, Baltazar F (2010) Histopathology 56:860
23. Rimoli MG, Rabaioli MR, Melisi D, Curcio A, Mondello S, Mirabelli R, Abignente E (2007) J Biomed Mater Res A 87A:156
24. Ghesti GC, Macedo JL, Parente VCI, Dias JA, Dias SCL (2007) Microporous Mesoporous Mater 100:27
25. Lutz W, Ruscher CH, Heidemann D (2002) Microporous Mesoporous Mater 55:193
26. Morris R (2007) In: Čejka J, van Bekkum H, Corma A, Schüth F (eds) Introduction to zeolite science and practice. Studies in surface science and catalysis, vol 168. Elsevier, Amsterdam
27. Breck DW, Flanigen EM (1968) Molecular sieves. Society of Chemical Industry, London, p 47